BioStudio -T

Cell Observation Device

Nikon's BioStudio-T was designed specifically for research applications in the field of regenerative medicine and stem cell biology and for use in cell manufacturing facilities. A compact live-cell imaging microscope, the BioStudio-T fits inside most incubators and is compatible with a variety of sterilization methods including vaporized H_2O_2. The fixed-stage, scanning lens system also provides a superior solution for long-term time lapse imaging and large image acquisition.

For more information on the BioStudio-T,
visit www.microscope.healthcare.nikon.com/biostudio-t

nikon-instruments-inc- nikoninstrumentsinc nikoninst nikoninstruments
Nikon Instruments Inc. | www.microscope.healthcare.nikon.com | nikoninstruments@nikon.net

STEM CELLS

TISSUE-SPECIFIC STEM CELLS

The Immunosuppressive Signature of Menstrual Blood Mesenchymal Stem Cells Entails Opposite Effects on Experimental Arthritis and Graft Versus Host Diseases

PATRICIA LUZ-CRAWFORD,[a,b,c] MARIA J. TORRES,[a] DANIELE NOËL,[b,c] AINOA FERNANDEZ,[a,d] KARINE TOUPET,[b,c] FRANCISCA ALCAYAGA-MIRANDA,[a,d] GAUTIER TEJEDOR,[b,c] CHRISTIAN JORGENSEN,[b,c,e] SEBASTIAN E. ILLANES,[a] FERNANDO E. FIGUEROA,[a] FARIDA DJOUAD,[b,c] MAROUN KHOURY[a,d]

Key Words. Menstrual-blood derived MSCs • Immunosuppression • CIA • GVHD

[a]Laboratory of Nano-Regenerative Medicine, Faculty of Medicine, Universidad de Los Andes, Santiago, Chile; [b]Inserm, U1183, Montpellier, France; [c]University Montpellier, Montpellier, France; [e]Clinical Immunology and Osteoarticular Diseases Therapeutic Unit, Lapeyronie University Hospital, Montpellier, France; [d]Cells for Cells, Santiago, Chile

Correspondence: Maroun Khoury, PhD, Av. San Carlos de Apoquindo 2500, Santiago, Chile. Telephone: +56226181956; Fax: +5622149468; e-mail: mkhoury@uandes.cl

Received February 20, 2015; accepted for publication September 14, 2015; first published online in STEM CELLS *EXPRESS* November 3, 2015.

1066-5099/2015/$30.00/0

http://dx.doi.org/10.1002/stem.2244

ABSTRACT

Recently, a noninvasive and highly proliferative stem cell population from menstrual blood called MenSCs has been identified. Despite their use in clinical studies, their immunomodulatory properties have not yet been investigated. In this context, we studied the immunosuppressive properties of MenSCs in comparison with the well-characterized bone marrow derived-MSCs (BM-MSCs). Using an in vitro proliferation assays, we showed that MenSCs displayed a lower suppressive effect on peripheral blood mononuclear cells and in particular on the proinflammatory $CD4^+IFN\text{-}\gamma^+$ and $CD8^+IFN\gamma^+$ cells than BM-MSCs. Moreover, compared to BM-MSCs, MenSCs activated with IFN-γ and IL-1β produced lower amounts of immunosuppressive factors such as IDO, PDL-1, PGE2, and Activin A and exhibited a substantial lower expression level of IFN-γ receptor subunits. In the collagen induced arthritis model, while BM-MSCs administration resulted in a potent therapeutic effect associated with a significant decrease of proinflammatory T cell frequency in the lymph nodes, MenSCs injection did not. In contrast, in the xeno-GVHD model, only MenSCs administration significantly increased the survival of mice. This beneficial effect mediated by MenSCs was associated with a higher capacity to migrate into the intestine and liver and not to their anti-inflammatory capacities. All together our results demonstrate for the first time that the therapeutic potential of MSC in the experimental xeno-GVHD model is independent of their immunosuppressive properties. These findings should be taken into consideration for the development of safe and effective cell therapies. STEM CELLS *2016;34:456–469*

SIGNIFICANCE STATEMENT

In the present study we report for the first time the immunosuppressive properties of MenSCs. We showed that they present lower immunosupressive properties compared to bone marrow-MSCs, evidenced by lower expression of several immunomodulatory factors, and the absence of beneficial effect in experimental arthritis model. However, their therapeutic effect was maintained in the xeno-GVHD model, but this was independent on their antiinflammatory capacities. Since the use of MenSC has being proposed for several clinical trials the information provided here raises the alertness for evaluating carefully their potential side effects, a key prerequisite for the development of safe cell therapies.

INTRODUCTION

Since Friedenstein and coworkers demonstrated that the osteogenic potential of bone marrow (BM) derived cells was associated with a restricted subpopulation of stromal cells, today well-described as mesenchymal stem cells (MSC), the field of cell therapy has expanded to become one of the most important lines of biomedical investigation [1, 2]. Furthermore, the discovery of the immunosuppressive properties of MSC [3] has widened the scope of these studies also promoting the search for new and less invasive sources for MSC isolation [4, 5]. Thus, the phenotypic and functional properties of MSCs from other sources such as placenta, adipose tissue, umbilical cord, synovium, tonsil, and dental tissues have been

reported [6–9]. More recently, a new source of MSCs isolated from menstrual fluids (MenSCs) has been identified [10–12]. Some of their practical advantages include the noninvasive method of their isolation, their easy expansion, high proliferative rate, potent angiogenic effect, migratory properties and hematopoietic stem cell support reported both in vitro and in vivo [13]. However, although the inhibitory effect of MenSCs on dendritic cells maturation has been reported [14] their immunosuppressive potential has not yet been fully investigated.

Currently, it is well-established that BM-MSCs display a potent regulatory effect on several immune cells including T cells, dendritic cells, and natural killer cells [15–17]. Although the mechanisms involved in BM-MSCs immunosuppressive effects are still under investigation, the suppressive role of prostaglandin E2, programmed cell death-ligand (PDL)-1, transforming growth factor-β1, interleukin (IL)-6, indoleamine 2,3 dioxygenase (IDO) has been described for human BM-MSCs [15, 18–20]. Some of these factors are expressed at a basal level by BM-MSCs while others are induced upon stimulation with proinflammatory cytokines, especially interferon (IFN-γ) solely or together with tumor necrosis factor (TNF-α) or IL-1β [21]. In line with this study, it has been reported that the inhibition of the IFN-γ receptor strongly reverses the suppressive properties of BM-MSCs on T-cell proliferation [22].

These immunomodulatory properties exerted by BM-MSCs have shown promising therapeutic effects promoting their use for the treatment of different autoimmune diseases like rheumatoid arthritis, systemic lupus erythematous, and graft versus host diseases (GVHD) [23–25]. Based on the encouraging preclinical studies, MSC-based therapies reached advanced stages of clinical investigation as many ongoing trials in patients have reached phases II and III; some of them with favorable results [26, 27].

In this study, we performed a broad evaluation of MenSCs immunomodulatory properties in vitro and in vivo, in comparison with BM-MSCs to improve our understanding of their biology and clinical potential. To that aim, we used two experimental models of autoimmune diseases, the collagen-induced arthritis (CIA) and the humanized xenograft versus host disease (GVHD).

Materials and Methods

Isolation and Characterization of BM-MSCs and MenSCs

For BM-MSCs isolation, BM from hip operated patients was used from four different donors while for MenSCs isolation, 3–5 ml of menstrual fluids were obtained from seven healthy donors from 18 to 45 years (Supporting Information Tables 1 and 2). Isolation and characterization were achieved as we previously described [13] according to the International Society for Cellular Therapy (ISCT) [28]. All the cells used in this study were harvested with the informed consent of the donor, and the study was approved by the Institutional Review Board of Universidad de los Andes, Chile. All the experiments were performed using MenSCs and BM-MSCs at early passages (P3–P7), and cells were routinely tested for mycoplasma.

Peripheral Blood Mononuclear Cell Proliferation Assays

Fresh peripheral blood mononuclear cells (PBMCs) from healthy donors where obtained after a density gradient centrifugation using the Ficoll-Paque Plus (Amersham, GE Healthcare, Piscataway, NJ, http://www.amersham.com) (1.077 g/ml). Briefly, PBMCs were stained with the carboxyfluorescein succinimidyl ester (CFSE) (Life Technology, Grand Island, NY, http://www.lifetech.com) and cultured in the presence or absence of BM-MSCs or MenSCs at different PBMC:MSC ratios (10:1 and 100:1) in contact or separated by a 0.4 μm transwell system (Corning Life Sciences, Union City, CA, http://www.corning.com/lifesciences) at 37°C, 5% CO_2 in the presence of 10 μg/ml of phytohemaglutinin (PHA) (Sigma-Aldrich, St Louis, MO, http://www.sigmaaldrich.com). After 72 hours, the proliferation of T cells was quantified by measuring the corresponding decrease in cell fluorescence by flow cytometry.

Analysis of T-Cell Subpopulation Frequency in PBMC In Vitro and In Vivo

Freshly isolated PBMCs from blood of healthy donors were cocultured in the presence or absence of BM-MSCs and MenSCs preactivated or not with 20 ng/ml of IFN-γ and 10 ng/ml of IL-1β at different PBMCs:MSCs ratios (10:1 and 100:1). After 72 hours of coculture, PBMC were stimulated for 4 hours with 50 ng/ml phorbolmyristate acetate (PMA) (Sigma-Aldrich) and 1 μg/ml ionomycin (Sigma-Aldrich) in the presence of Brefeldin A (Biolegend San Diego, CA, http://www.biolegend.com).

For surface staining, cells were incubated with antibodies against human CD4, CD8 and CD25 (Biolegend) in the dark at 4°C for 20 minutes and fixed at 4°C with the forkhead box P3 (FoxP3) staining buffer set (eBioscience, San Diego, CA, http://www.ebioscience.com). For intracellular staining, cells were then incubated for 30 minutes with antibodies against IFN-γ-PE, IL-17-Percp5.5, IL-10-PE (BD Pharmingen, San Diego, CA, http://www.bdbiosciences.com/index[lowen]us.shtml) and RAR-related orphan receptor gamma (ROR-γT)-APC and FoxP3-FITC (eBioscience). Data were acquired using a FACS Canto II and analyzed with the BD FACSdiva (BD Pharmingen) and the FlowJo software (Tree Star, Inc., http://www.flowjo.com).

Real Time Quantitative PCR Analysis

Total RNA from BM-MSCs and MenSCs activated during 48 hours in the presence or absence of 20 ng/ml IFN-γ or IFN-γ with 10 ng/ml IL-1β were extracted using the RNeasy mini kit (Qiagen S.A., Valencia, CA, http://www1.qiagen.com). RNA (500 ng) was reverse transcribed using the M-MuLV Reverse Transcriptase (New England BioLabs, Ipswich, MA). Quantitative polymerase chain reaction (PCR) was performed using the Brilliant II SYBR Green QPCR Master Mix according to the manufacturer recommendations (Agilent Technologies, La Jolla, CA, http://www.agilent.com) in the Mx3000P system (Stratagene, Agilent Technologies, La Jolla, CA). Specific primers for IDO and Cox 2 were designed using the Primer-Blast program (Supporting Information Table 3). Data were expressed as relative mRNA level of specific gene using the $2^{-\Delta Ct}$ method and normalized with the Beta 2 microglobulin housekeeping gene.

Assessment of the IDO Activity

BM-MSCs and MenSCs cells were stimulated with 100 ng/ml of IFN-γ during 48 hours in complete Dulbecco's modified Eagle's medium (DMEM) medium in the presence of 100 μg/ml of L-tryptophan (Sigma-Aldrich). IDO enzyme activity was measured determining the kynurenine concentration in the cell supernatant as previously reported [29].

Activin A, PDL1, CXCR4, and IFNGR1 Quantification

Activin A was quantified in the supernatants of BM-MSCs and MenSCs activated for 48 hours in the presence or absence of 20 ng/ml IFN-γ or IFN-γ with 10 ng/ml IL-1β using an enzyme-linked immunosorbent assay from R&D Systems (R&D Systems, Minneapolis, MN, http://www.rndsystems.com) following the manufacturer instructions. For PDL-1, CXCR4, and IFNGR1 detection, BM-MSCs or MenSCs with or without activation were collected and stained with specific antibodies (BD Pharmingen) and analyzed by flow cytometry.

CIA Induction

Adult male DBA/1 mice aged between 9 and 10 weeks were immunized with 100 μg of Chicken Collagen II (ChCII), (Thermoscientific, Rockford, IL) emulsified with an equal volume of Freund's complete adjuvant in the presence of 40 μg of *Mycobacterium tuberculosis* (Difco, Le Pont-de-Claix, France), followed by a boost injection of the ChCII emulsion in Freund's incomplete adjuvant at day 21. Then 5×10^5 BM-MSCs or MenSCs or saline were injected intravenously at day 18 and 24 postimmunization. The development and progression of arthritis symptoms were assessed every 2–3 days by measuring the paw swelling of the hind paw and evaluating the clinical score using the macroscopic scale as previously described [30].

Quantification of Cytokines Produced by PBMCs, Lymph Nodes Cells, and Splenocytes of Mice

PBMCs from all CIA mice groups were isolated at different time points after MSC injection (Day 21, 28 and 32 postimmunization) and cultured for 48 hours with 100 ng/ml of lipopolysaccharid (LPS). At euthanasia, draining lymph nodes and splenocytes from the different groups were activated in the presence of 25 μg/ml chicken collagen II for 48 hours. Supernatants were collected and stored at −80°C. Murine IL-5, IL-6, IL-10, IL-13, TNF-α were quantified using a R&D Systems kit (R&D Systems) following the manufacturer instructions.

Experimental Xenogenic GVHD Model

For the induction of GVHD, 8–10 weeks old NOD-scid IL2rγnull (NSG) mice were irradiated using a dose of 1.5 Gy at the Chilean Commission for Nuclear Energy Facilities. At 24 hours post-irradiation, mice were injected through the tail vein with 12×10^6 human PBMCs obtained from the buffy coat of healthy donors (Centro Metropolitano de Sangre y Tejidos, Servicio Metropolitano Sur Oriente, Santiago, Chile). This was followed by an immediate intraperitoneal injection of 1×10^6 BM-MSCs or MenSCs. The onset of the GVHD occurs typically around day 7 post-PBMCs injection. The GVHD monitoring was done by weighing the animals on daily basis. Euthanasia of the mice was performed at days 8 and 14. Target organs were harvested from each group for specific human RNA expression levels of β-2 microglobulin, Foxp3, IL-10, IL-6, Neurophilin 1, IFN-γ, vascular endothelial growth factor (VEGF), and hepatic growth factor (HGF) (Supporting Information Table 3). Cells from the peripheral blood and spleen were also isolated. An immunophenotypic analysis using antibodies against mouse CD45, human CD45, CD4, and CD8 was performed to detect the presence of human lymphocytes within the mouse tissue samples by fluorescence-activated cell sorting (FACS).

Histopathological Analysis

The presence of GVHD was assessed by morphologic analysis of the small intestine. The samples were harvested from mice at day 8 post-GVHD and fixed in 10% formalin (Sigma). Following fixation, the specimens were embedded in paraffin, cut into 5-μm-thick sections and stained with hematoxylin and eosin. Slides were analyzed in a blinded fashion to assess the severity of GVHD. Pictures were obtained using the Nanozoomer (Hamamatsu Photonics K.K, Hamamatsu, Japan) and the analysis was made with the NDP scan 2.5 program (Hamamatsu Photonics K.K.). For histopathological quantification in the small intestine, the epithelial damage index was calculated using the parameters as previously described [31].

Migratory Assay

BM-MSCs and MenSC (2×10^4) cells were stained with cell tracker red (Life Technology) for 40 minutes and added to the upper chamber of a Fluoroblok cell cultured insert (8-μm pore size, Corning Costar, NY) in serum-free medium. The migratory stimulus corresponds to media supplemented with 10% fetal bovine serum (FBS). After 6, 12, and 24 hours, the cells that have migrated at the lower surfaces of the membranes were fixed and stained with 4′,6-diamidino-2-phenylindole (DAPI). Photographs were taken using a fluorescence microscope (Axiovert 200, Zeiss), and the number of cells that have migrated was determined using the Image J software.

Scratch Assay

A straight-line scratch was performed using a 10 μl pipette tip over a confluent monolayer of BM-MSCs or MenSCs plated in a six-well plate. Then, cells were washed with PBS to remove detached cells and incubated in DMEM 2% FBS media for 24 hours. Photographs were acquired at different time laps using a phase-contrast microscope, and the number of migrating cells into the ruptured area was quantified using the ImageJ analysis software.

Biodistribution Studies

For intraperitoneal administration, 10^6 BM-MSCs or MenSCs were resuspended in 200 μl of PBS and injected in NSG mice at 24 hours post-irradiation. Twenty four hours and eight days after MSC injection the liver, the heart, the spleen, and the intestine were collected in RLT buffer (Qiagen S.A.) and frozen at −80°C. For intravenous administration, 5×10^5 BM-MSCs or MenSCs were injected via tail vein at day 18 and 24 after collagen type II immunization of DBA mice. 24 hours after the second MSC injection the spleen, lymph nodes, ankles, knees, and lungs were collected and frozen at −80°C.

Tissues were disrupted using an ultraturrax homogenizer, and DNA or RNA extractions were achieved on 30 mg of tissue suspension using the AllPrep DNA/RNA Mini Kit (Qiagen S.A.) and quantified using a spectrophotometer (Nanodrop, Labtech, Palaiseau). Real time quantitative PCR (RT-qPCR) was

performed using 0.05 μM primers for human *arthrobacter luteus* (ALU) (hALU) or 0.5 μM for murine Actin (mActin) (Supporting Information Table 2). PCR conditions and human Alu Sequences were setting as previously described [32]. Standard curves were made by adding 10-fold serial dilutions of either human BM-MSCs or MenSCs in murine MSCs (10^6 total cell number). Results were expressed as the number of cells per 100 mg of either human BM-MSCs or MenSCs per organ, and limit of detection was estimated to be 0.005% human cells of total injected cells.

Statistical Analysis

Results are expressed as the mean ± SEM. All in vitro experiments were performed for at least three independent times and using three or four BM-MSCs and seven MenSC donors each time. For the proliferation assay and study of T-cell subpopulations on PBMCs after cocultured with either BM-MSCs or MenSCs the experiment was repeat at least three times and using three different BM-MSCs, seven MenSCs, and three PBMCs donors each time. For the in vivo studies, 8–10 animals were used for each experimental group. For GVHD model, the experiment was repeated at least five times using two different donors for BM-MSCs and MenSC. For CIA model we performed the experiment two times using two different donors. *p* values were generated using nonparametric analysis using the Mann–Whitney test to compare between two groups. For survival analysis data were plotted by the Kaplan–Meier method and analyzed by the log rank test. *p* values $< .05$ (*), $p < .01$ (**), or $p < .001$ (***) were considered statistically significant. All the analyses were performed using the Graph-Pad Prism 6 software (Graphpad, San Diego, CA).

Results

MenSCs Display a Reduced Anti-Inflammatory Effect on T-Cell Proliferation and Phenotype Compared to BM-MSCs

The immunosuppressive properties of MenSCs were tested in vitro by assessing their capacity to modulate the proliferative response of CFSE-labeled PBMCs upon PHA stimulation (Fig. 1A). Cells were cocultured at 1:10 and 1:100 MSC to PBMC ratios. MenSCs exhibited a similar inhibitory effect on T-cell proliferation compared to BM-MSCs at the 1:10 ratio (Fig. 1A). However, while BM-MSCs still exert a suppressive potential when cultured at a lower ratio (1:100), MenSCs showed a stimulatory effect on T cells (Fig. 1A). Taking into account the suppressive functions of MSCs on pathogenic T-cell subsets such as Th1, Th17, T-CD8 cytotoxic lymphocytes, and regulatory T cells (Treg), we investigated the frequency of these T-cell populations. For that purpose, 72 hours post-coculture with BM-MSCs or MenSCs, PBMCs were treated during 4 hours with PMA/Ionomycin in the presence of Brefeldin A in order to determine the cytokine production profiles by FACS. Then, the frequency of CD8 cytotoxic lymphocytes, Th1, Th17 cells, and regulatory T cells was assessed. Compared to BM-MSCs, we observed a significantly lower suppressive effect of MenSCs on IFN-γ secreting cells including both $CD4^+$ (Th1) and $CD8^+$, when cocultured at a MSCs:PBMCs cell ratio of 1:100 (Fig. 1B). In contrast, no significant difference was observed on the percentage of Th17 cells (Fig. 1C). At the cell ratio 1:100, MenSCs displayed a reduced capacity to generate $CD4^+IL4^+IL10^+$ T cells when cocultured with PBMCs compared to BM-MSCs (Fig. 1D). No difference between MSCs was observed on classical Treg cells (data not shown). Moreover, we observe the same increase in proliferation of T-cells at a 1:100 ratio when we coculture MenSCs with PBMCs from the same donor (data not shown). These results demonstrate that MenSCs exert less immunosuppressive effects in vitro than BM-derived MSCs.

MenSCs Display a Lower Capacity to Produce Suppressive Factors Than BM-MSCs

We then compared the capacities of BM-MSC and MenSCs to express the well-described suppressive molecules involved in BM-MSCs immunosuppressive properties. For that purpose, we studied the production of different molecules already associated to the suppressive effect of MSCs. Our results showed that MenSCs expressed significantly lower levels of Cox-2 and IL-6 as well as a lower secretion of Activin A or IDO activity compared to BM-MSCs under both basal and activated conditions (Fig. 2A, 2B). Then, we assessed the expression level of PDL-1, described to play a major role in regulating the immune response. While we observed a significant increase of PDL-1 expression in BM-MSCs upon stimulation, we did not observe any change in MenSCs (Fig. 2C). This lower expression level of suppressive factors produced by MenSCs was associated with a significantly lower expression level of the IFNγ-R1 and -R2 compared to BM-MSCs (Fig. 3A). Thus, in order to functionally define the role of proinflammatory cytokines in the suppressive signature of MenSCs, we performed a proliferation assay in the presence or absence of both BM-MSCs and MenSCs preactivated or not with IFN-γ and IL-1β. Our results showed that while preactivated BM-MSCs significantly inhibit the proliferation of T cells at a MSC:T ratio of 1:100, the preactivation of MenSCs did not change their suppressive capacities (Fig. 3B), suggesting that MenSC are less activated by proinflammatory molecules. Altogether these data suggest that the lower immunomodulatory effect of MenSCs compared to BM-MSCs might be due to a reduced expression of suppressive molecules both under basal or activated conditions.

MenSCs Fail to Exert a Therapeutic Effect in the CIA Model

The therapeutic effect mediated by MSCs in experimental autoimmune diseases is mainly due to their immunosuppressive properties leading to a decrease of the proinflammatory response [25, 33]. The discrepancy observed in vitro between BM-MSCs and MenSCs suggests that these cells might exhibit different therapeutic effect in vivo. We thus compared the effect of BM-MSCs and MenSCs in experimental models of inflammatory diseases. First, we used the CIA model to address the anti-inflammatory potential of MenSCs in vivo. While the systemic injection of BM-MSCs significantly reduced the progression of arthritis (Fig. 4A), MenSCs did not (Fig. 4A). Assessing at the immunological parameters, we showed that BM-MSCs reduced the secretion of TNF-α by activated PBMC, while MenSCs injection induced a twofold increase of TNF-α expression at day 27 compared to the control group (Fig. 4B). No significant difference was observed on IL-10, IL-6, and IL-1β secretion levels (data no shown). At euthanasia, the frequency of the different proinflammatory T-cell populations was analyzed in the draining lymph nodes and spleens. Both

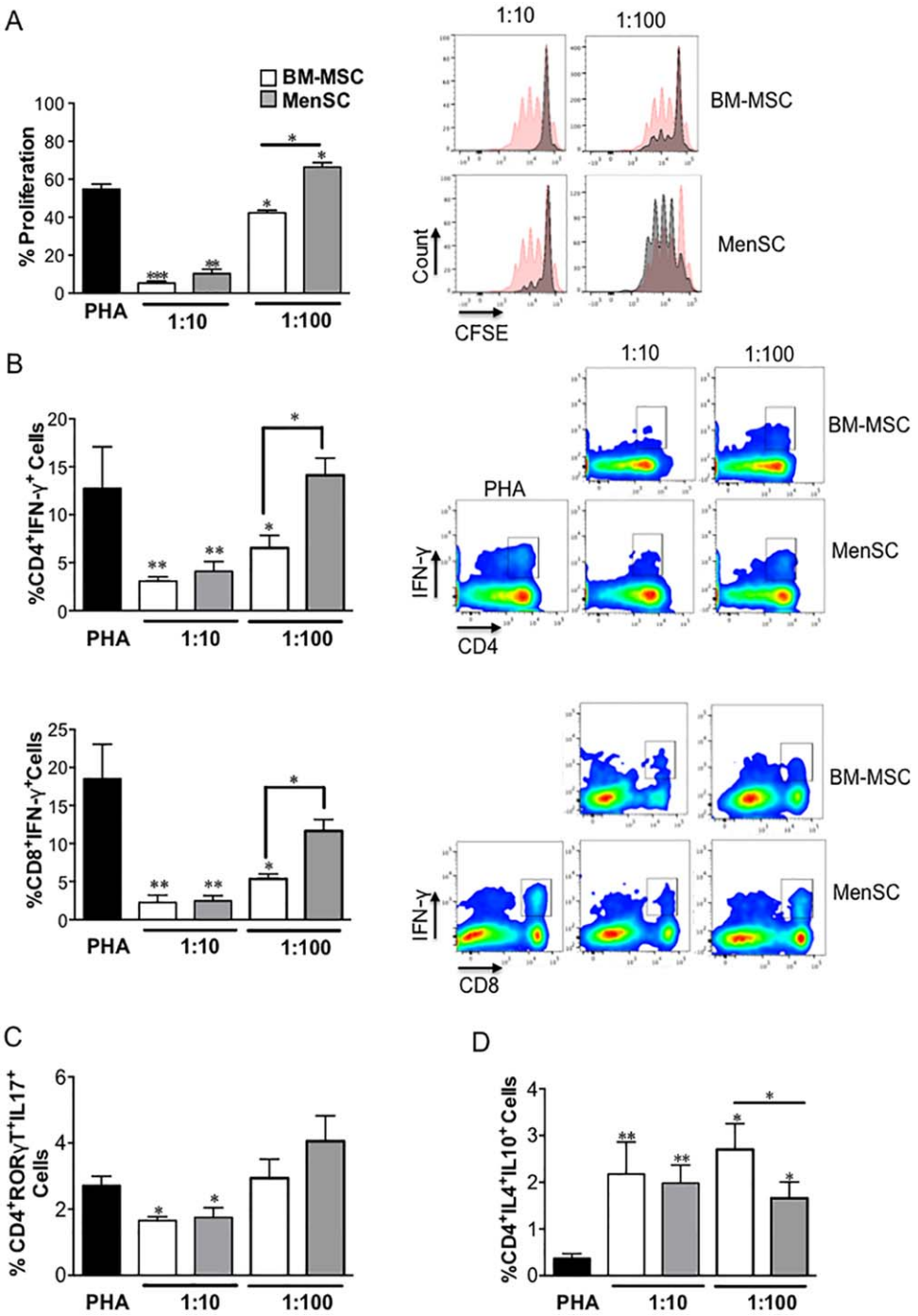

Figure 1. MenSCs display less suppressive capacities to inhibit proinflammatory T cells than BM-MSCs. **(A)**: Allogeneic activated peripheral blood mononuclear cells (PBMC) labeled with CFSE were cocultured with or without BM-MSCs and MenSCs at different MSCs:PBMC ratios (1:10 and 1:100 MSC:PBMC) (left: representative CFSE proliferation panel) (light color histogram: activated PBMCs; dark color histogram: activated PBMC with either BM-MSCs or MenSCs). **(B, C)**: Th1, CD8, and Th17 proinflammatory subset analysis from coculture of BM-MSCs and MenSCs with allogeneic-activated human PBMC at different MSCs:PBMC ratios. **(D)**: Anti-inflammatory $CD4^+IL4^+IL10^+$ cells analysis under the same culture conditions. Results are represented as mean ± SEM of at least five independent experiments using at least three different donors for PBMC, MenSC, and BM-MSCs each time (*, $p < .05$; **, $p < .01$; ***, $p < .005$). Abbreviations: BM-MSCs, bone marrow-derived mesenchymal stem cells; CFSE, carboxyfluorescein succinimidyl ester; IFN, interferon gamma; IL, interleukin; MenSC, MSCs isolated from menstrual fluids; PHA, phytohemaglutinin; RORγT, RAR-related orphan receptor gamma.

BM-MSCs and MenSCs significantly reduced the frequency of CD8 and Th1 cells but to a significantly lesser extent for MenSCs (Fig. 4C; Supporting Information Fig. 4). Moreover, only BM-MSC treatment significantly inhibited the frequency of proinflammatory Th17 cells in lymph nodes (Fig. 4C). Supernatants from activated cultures of LNC from mice treated with BM-MSCs or MenSCs exhibited significantly higher concentrations of the anti-inflammatory cytokines IL-5, IL-10, and IL-13 compared to CIA control mice (Fig. 4D). Then, we quantified the proinflammatory cytokines and found a

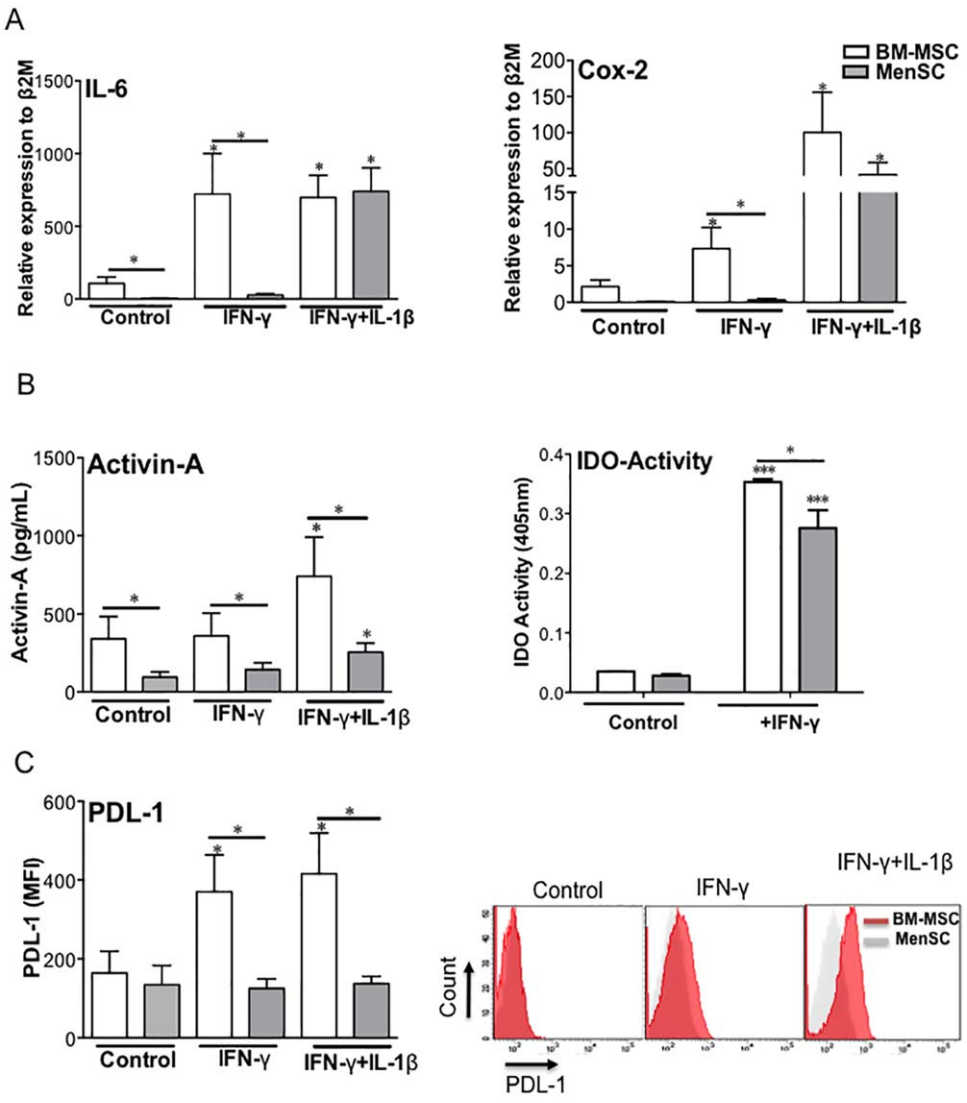

Figure 2. MenSCs are less responsive to cytokine activation and express less immunosuppressive molecules compared to BM-MSCs. **(A)**: Quantification of Cox 2, IL-6, and IDO by quantitative polymerase chain reaction. **(B)**: Activin A secretion levels by ELISA and IDO activity measured by Kynurenine production. **(C)**: PDL-1 expression levels by fluorescence-activated cell sorting. Activin A secretion and IDO activity were quantified in the supernatants of MSC and MenSCs cultured in the presence or absence of 20 ng/ml of IFN-γ or 100 ng/ml of IFN-γ, respectively, alone or with 10 ng/ml of IL-1β. PDL-1, Cox-2, IL-6, and IDO expression levels were quantified on BM-MSCs or MenSCs under the same culture conditions described below. Results are represented as mean $\pm$ SEM of at least three independent experiments using each time at least three different MenSCs and BM-MSC donors. *, $p < .05$; **, $p < .01$; ***, $p < .005$ with respect to the MSCs control group without proinflammatory cytokines treatment. Abbreviations: BM-MSCs, bone marrow-derived mesenchymal stem cells; IL, interleukin-1β; IFN, interferon; IDO, indoleamine 2,3 dioxygenase; MenSC, MSCs isolated from menstrual fluids; PDL-1, programmed cell death-ligand; β2M, Beta 2 microglobulin.

significant increase of TNF-α and IL-6 produced by splenocytes isolated from MenSCs injected mice compared to both control and BM-MSCs mice (Supporting Information Fig. 4). Taken together, all the immunological and clinical parameters demonstrated the inability of MenSCs to suppress the inflammatory response and exert a beneficial effect in the experimental CIA model.

MenSCs Increased the Survival Rate of GVHD Mice Independently of the Degree of Inflammation

We then investigated whether the low immunomodulatory potential of MenSCs may be sufficient to inhibit the inflammation in other clinical indications. To that aim, we used the humanized-GVHD mouse model to evaluate the therapeutic potential of MenSCs. Mice were irradiated before the administration of human PBMCs alone (control group) or together with BM-MSCs or MenSCs. Six days post-GVHD induction, while a loss of weight was recorded in the control group, the groups treated with either BM-MSCs or MenSCs did not display any significant weight change (Fig. 5A). Although both MSC treated groups exhibited an improvement in survival that was significant only after MenSCs injection (Fig. 5A). In contrast, in the spleen of MenSCs treated group compared to the BM-MSCs treated group, a significantly higher number of human CD45$^+$ cells was detected (Fig. 5B) suggesting that MenSC were not able to inhibit the activation of human

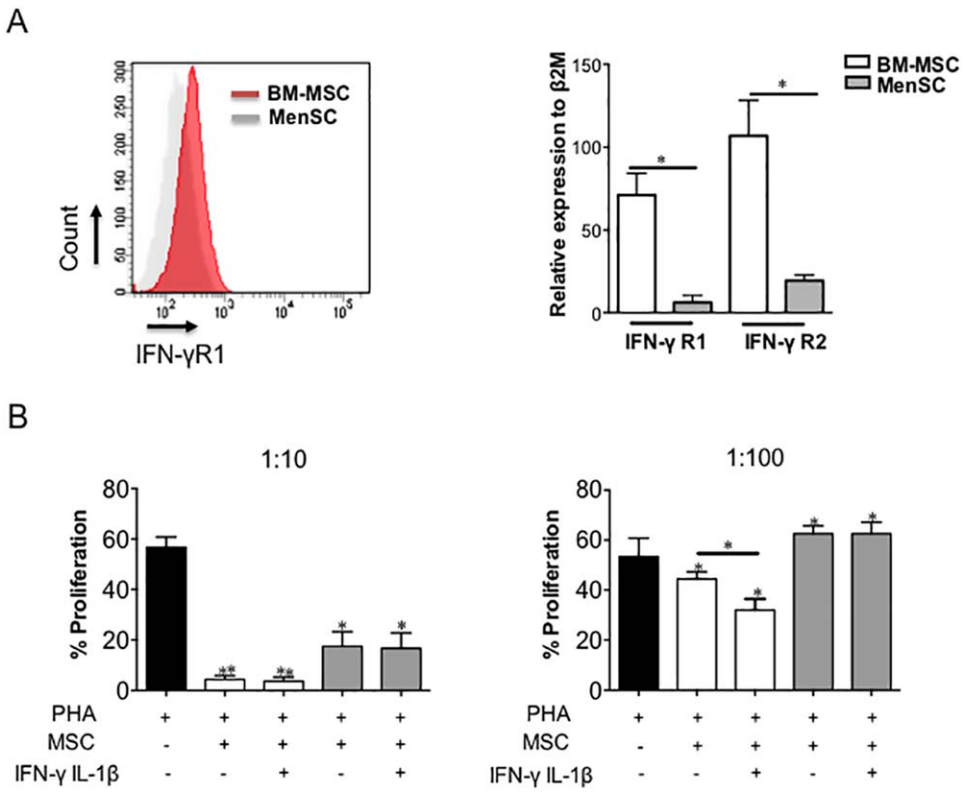

Figure 3. MenSCs showed a lower expression level of IFN-γ receptor subunits and did not increase their suppressive effect upon preactivation. **(A)**: IFN-γ receptor expression in both BM-MSCs and MenSCs quantified by fluorescence-activated cell sorting and quantitative polymerase chain reaction. **(B)**: Allogeneic activated peripheral blood mononuclear cell (PBMC) labeled with carboxyfluorescein succinimidyl ester were cocultured with or without BM-MSCs and MenSCs preactivated or not with IFN-γ and IL-1β at different MSCs:PBMC ratios. Results are represented as mean $\pm$ SEM of at least three independent experiments using at least three different donors for MenSCs and three different donors for BM-MSC. p values referred to activated PBMC without MSCs. Abbreviations: BM-MSCs, bone marrow-derived mesenchymal stem cells; IFN, interferon; IL, interleukin; MenSC, MSCs isolated from menstrual fluids; PHA, phytohemaglutinin; β2M, Beta 2 microglobulin. *$p < 0.05$; **$p < 0.01$.

T cells. Moreover, no difference was observed in the percentage of $CD45^+CD4^+$ cells in all groups (Fig. 5B) while the frequency of human CD45+CD8 + effector cells was only decreased in the spleen of mice treated with BM-MSCs (Fig. 5C). The quantification of proinflammatory mediators revealed a significant increase of IFN-γ that paralleled a decrease of Foxp3 expression level in splenocytes of MenSCs treated mice (Fig. 5D). Interestingly, we measured high expression levels of IL-6 and lower expression of Foxp3 and NRP-1 in the PBMC of MenSCs treated group (Supporting Information Fig. 5). This data suggest that MenSC impaired the proliferation of natural regulatory T cells in circulation (Supporting Information Fig. 5B) that could be associated with the increased percentage of human T-CD8 cells that we observed in the spleen.

Histological analysis of the intestine harvested from untreated mice revealed the presence of damages with villous blunting (Fig. 6A) and a higher epithelial damage index than those recorded in treated mice (Fig. 6A). Interestingly, we observed a significantly higher expression level of human HGF and VEGF in the liver of animals treated with MenSCs compared to the mice that have received BM-MSCs. These results suggest that MenSCs exert a beneficial effect in the experimental GVHD model, which was not associated with their capacity to suppress inflammation.

MenSCs Exhibit Higher Migratory Capacities Than BM-MSC

Finally, we investigated the possible mechanisms involved in the therapeutic effect of MenSCs in the experimental GVHD model. For that purpose, we assessed the migratory capacity of both BM-MSCs and MenSCs since the ability of MSC to migrate into the damage tissue is one of the main mechanisms that contribute to tissue regeneration [34]. Since MSCs overexpressing the migratory molecule CXCR4 displayed a significantly increased migratory capacity in vitro together with a decreased mortality rate in a GVHD model [35] we decided to study the expression level of CXCR4 in BM-MSCs and MenSCs. Our results showed that a higher percentage of CXCR4 + cells was found in the MenSC population compared to BM-MSCs (Fig. 7A). Then in vitro, we evaluated the migratory capacity of MenSCs and BM-MSCs either using a transwell or in a wound-healing assay. We observed that MenSCs migrated more rapidly than BM-MSCs, resulting in a significantly higher number of migrating cells in the lower chamber of the transwell membrane after 24 hours of culture (Fig. 7B). In the same line, in the wound-healing assay, we showed that MenSCs were able to close the wounded area faster than BM-MSCs (Supporting Information Fig.6). We then looked at the biodistribution of BM-MSCs and MenSCs in NSG irradiated

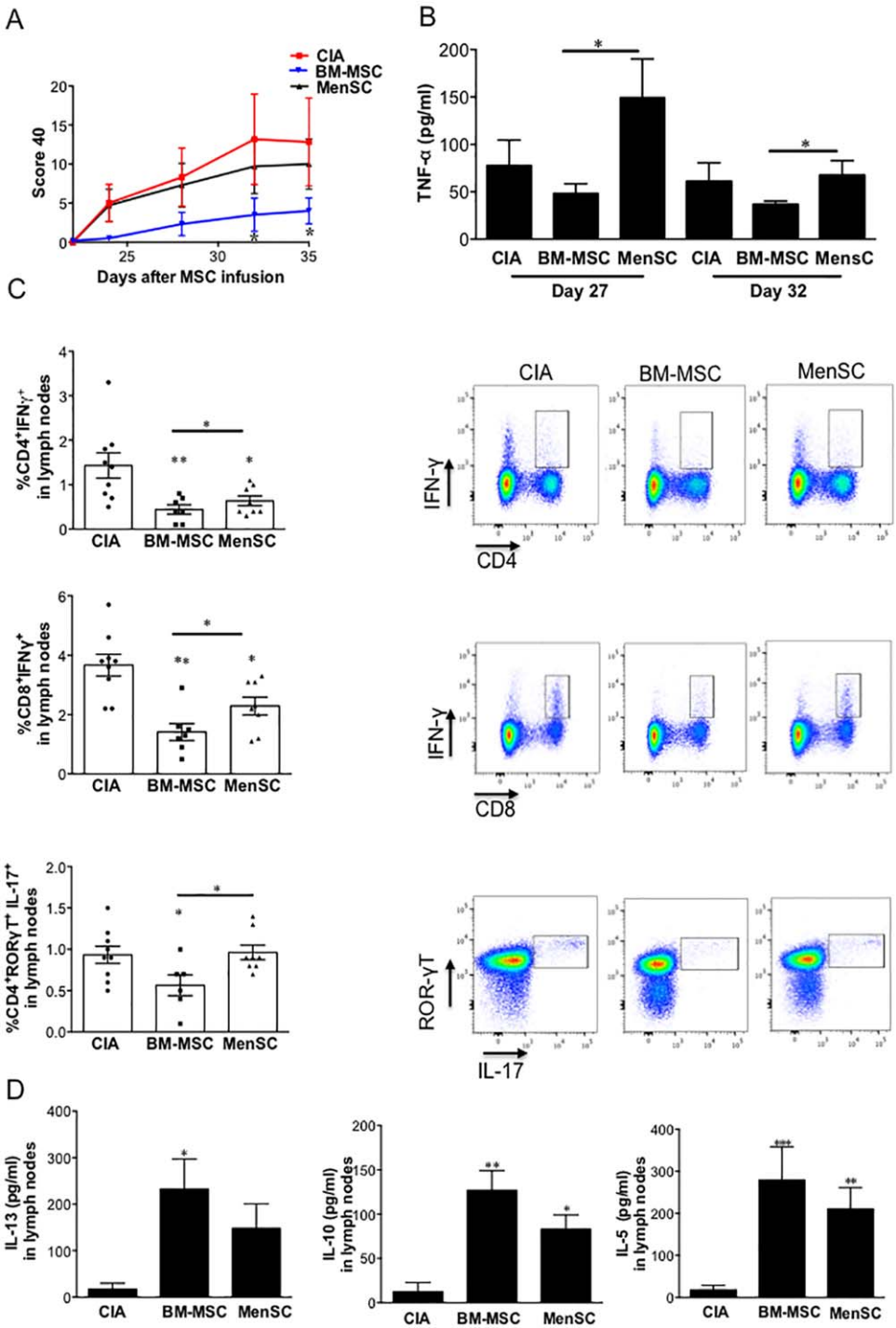

Figure 4. MenSCs do not show therapeutic benefit in the experimental arthritis model. DBA mice were immunized with chicken collagen type II emulsified with Freund's complete adjuvant. On day 18 and 24 after immunization 1×10^6 BM-MSCs and MenSCs were injected into the tail vain. **(A)**: Clinical score of arthritis was determined every each day after the second cell injection. **(B)**: TNF-α was detected in the supernatants of activated peripheral blood mononuclear cell (PBMC) at different time points of arthritis progression. **(C)**: The frequency of Th1, CD8 secreting IFN-γ, and Th17 cells was determining in draining lymph nodes (dLNs) of mice from the different experimental groups at day of euthanasia. **(D)**: IL-5, IL-10, and IL-13 were detected after 48 hours of dLNs activation with 25 μg/ml of chicken collagen II. (A–D), scale bars show the mean ± SEM of seven to nine different mice per experimental group. (C): Representative dot plot of flow cytometry data show the expression of IFN-γ gated on the CD8 cells and IFN-γ and RORγT IL-17 producing cells gated on CD4 cells from one of two independent experiments. *, $p < .05$; **, $p < .01$; ***, $p < 0.005$ with respect to the non treated group. Abbreviations: BM-MSCs, bone marrow-derived mesenchymal stem cells; CIA, collagen induced arthritis; IFN, interferon; IL, interleukin; MenSC, MSCs isolated from menstrual fluids; ROR-γT, RAR-related orphan receptor gamma.

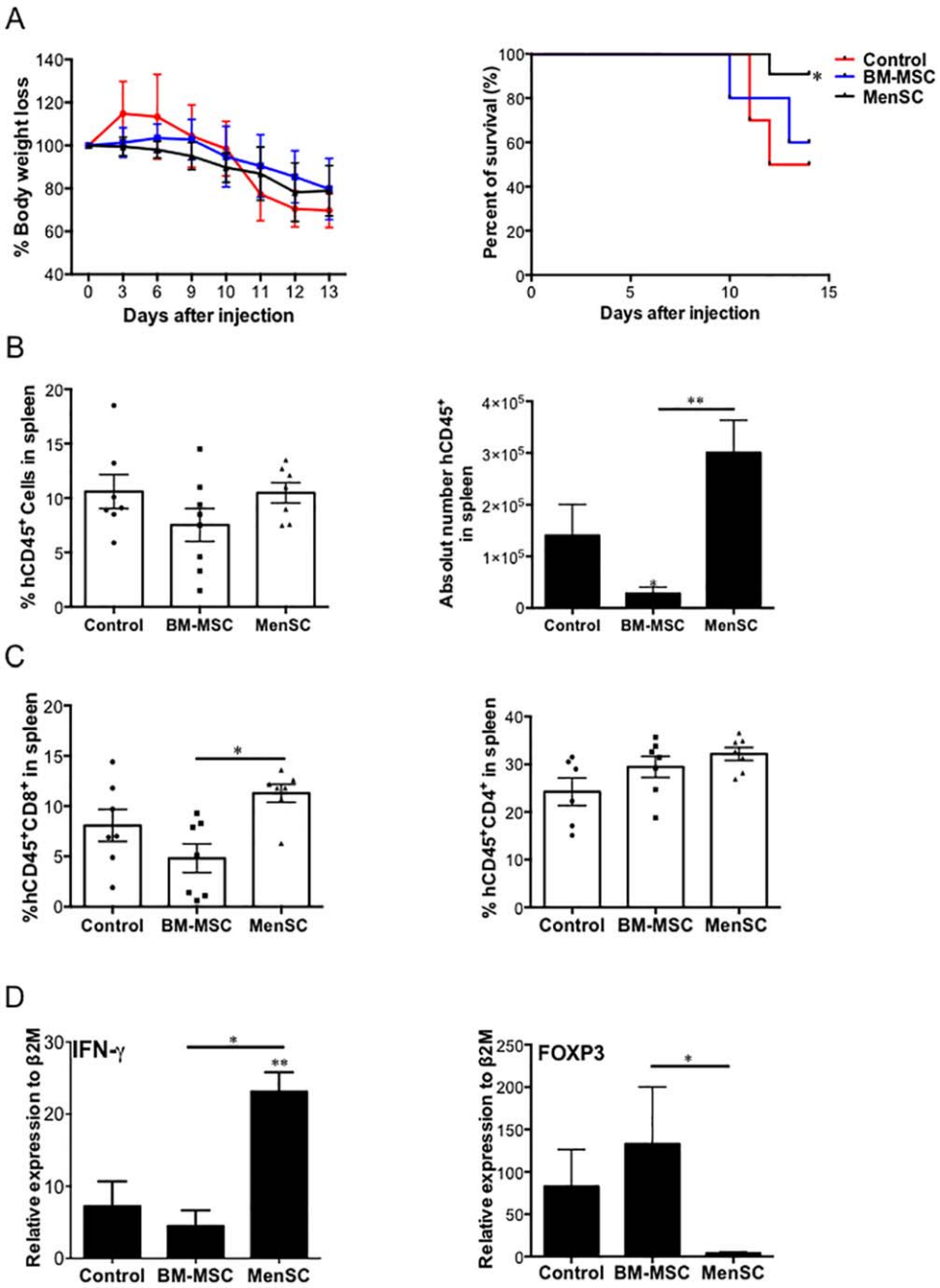

Figure 5. MenSCs increased the number of CD45 + cells and the expression levels of proinflammatory mediators in xeno-GVHD (graft versus host disease) while showing a higher survival. **(A)**: Weight loss and survival of mice were determined daily. **(B)**: The percentage and absolute number of human CD45 cells were quantified by fluorescence-activated cell sorting (FACS). **(C)**: The percentage of CD4 and CD8 cells was quantified by FACS. **(D)**: Human IFN-γ and Foxp3 were quantified by quantitative polymerase chain reaction. All data were quantified at day 8 after GVHD induction in the spleen of animals from all the different experimental groups. Bars show the mean $\pm$ SEM of 7–10 different mice per experimental group. The experiment is representative of four independent experiments for survival while three independent experiments for day 8 analysis. *, $p < .05$; **, $p < .01$ referred to the nontreated group. Abbreviations: BM-MSCs, bone marrow-derived mesenchymal stem cells; MenSC, MSCs derived from menstural fluids; IFN, interferon; β2M, Beta 2 microglobulin.

mice following intraperitoneal injections (IP). One day after the injection, we detected both BM-MSCs and MenSCs in the liver of 4/5 mice while in the intestine, spleen, and heart in 5/5 of NOD irradiated mice (Fig. 7C). Interestingly, a significant difference in the number of MenSCs present in the liver, the spleen and the intestine was detected in comparison to BM-MSCs (Fig. 7C). While this significant difference between the two groups was not maintained at day 8 postinfusion, the number of BM-MSCs in the liver decreased by eightfold while MenSCs numbers decreased by only 2.5-fold (Fig. 7D). Interestingly, the biodistribution assay using the CIA model showed the presence of MSCs in the lung of all the mice that have

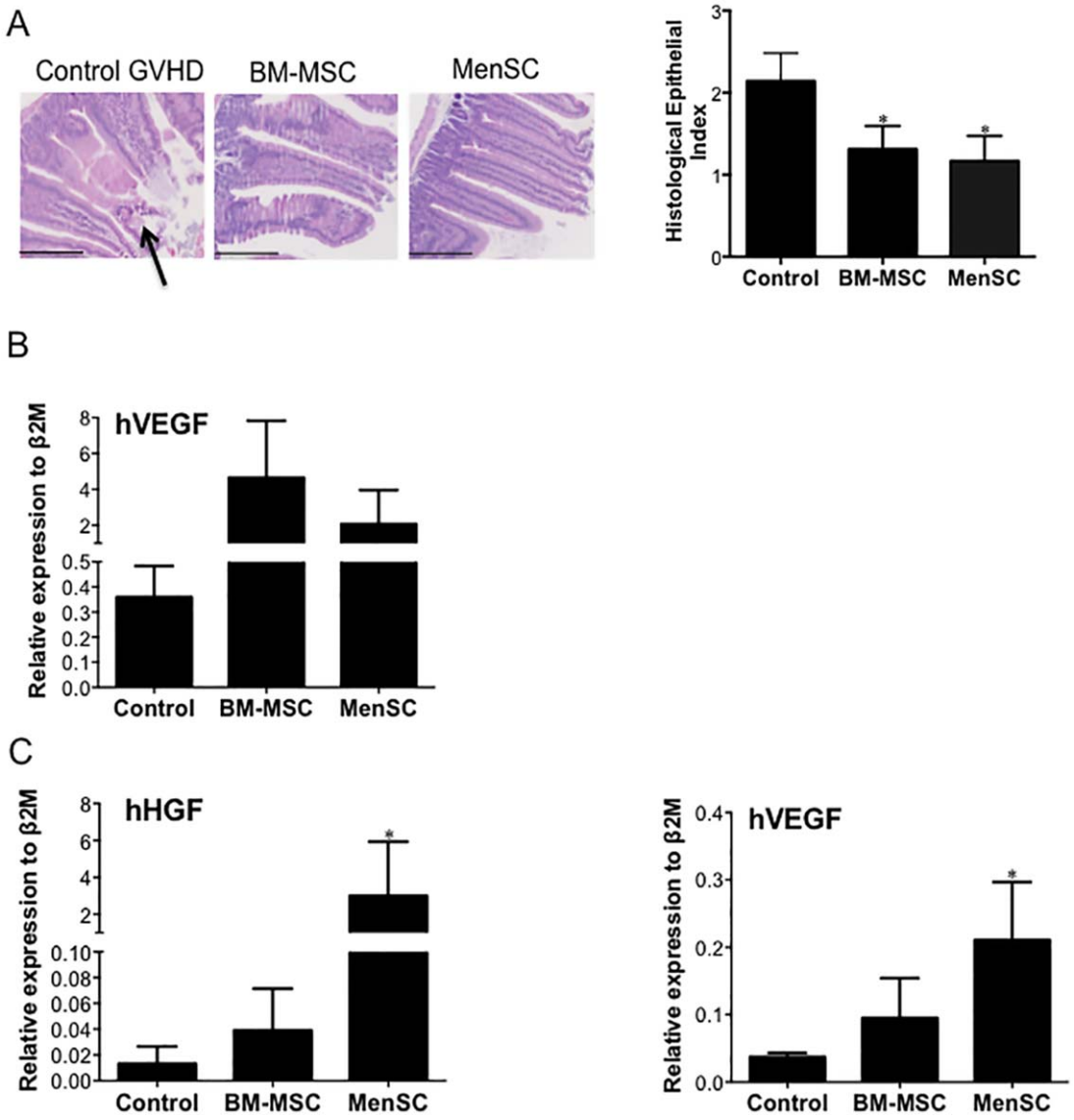

Figure 6. Tissue protective effects of MenSCs are mediated through the secretion of growth factors. **(A)**: Histological analysis of the intestines of mice at day 8 (magnification of $\times$ 200, scale bar = 50 μm). **(B)**: Human VEGF quantification in the intestine by real time quantitative polymerase chain reaction (RT-qPCR). **(C)**: VEGF and HGF quantification in the liver by RT-qPCR. All the quantifications were performed at day 8 after GVHD induction. Bars show the mean $\pm$ SEM of six to eight different mice for all the different experimental groups. p values referred to the nontreated group. Abbreviations: BM-MSC, bone marrow-derived mesenchymal stem cells; GVHD, graft versus host disease; hHGF, human HGF; HGF, hepatocyte growth factor, *$p < 0.05$; vascular endothelial growth factor (hVEGF), human VEGF; MenSC, MSCs isolated from menstrual fluids; VEGF, vascular endothelial growth factor; β2M, Beta 2 microglobulin.

been treated with MenSCs and only in 50% of the mice treated with BM-MSCs. Moreover, MSCs have been found in the lymph nodes of 75% of the mice treated with MenSCs and in only 25% of the mice treated with BM-MSCs. All together these data suggest that the higher therapeutic effect of MenSCs in the GVHD model compared to BM-MSCs might be due to their higher rate of migration, survival and homing into the different damage tissues in vivo.

Discussion

In this work, we study the immunosuppressive properties of MenSCs, which have so far been poorly investigated. We first addressed whether MenSCs possess immune-privileged properties and showed that such as BM-MSCs, MenSCs express low levels of histocompatibility antigen (HLA)-B, -C, and do not express HLA-DR. A very similar immunophenotype was shared with BM-MSC suggesting that MenSC may also be able to escape immune recognition. However a lower expression levels on Toll like receptor 3 and 4 expression was observed on MenSCs, suggesting that the immunomodulation exerted by these cells might differ to BM-MSCs. Then, we assessed the effect of MenSCs on the proliferation of activated PBMCs. While MenSCs were as efficient as BM-MSCs to suppress T cell proliferation at the 1:10 cell ratio, a lower suppressive effect of MenSCs was observed at the 1:100 ratio. Nikoo et al. [36] have previously described that MenSCs exhibit a dual anti-

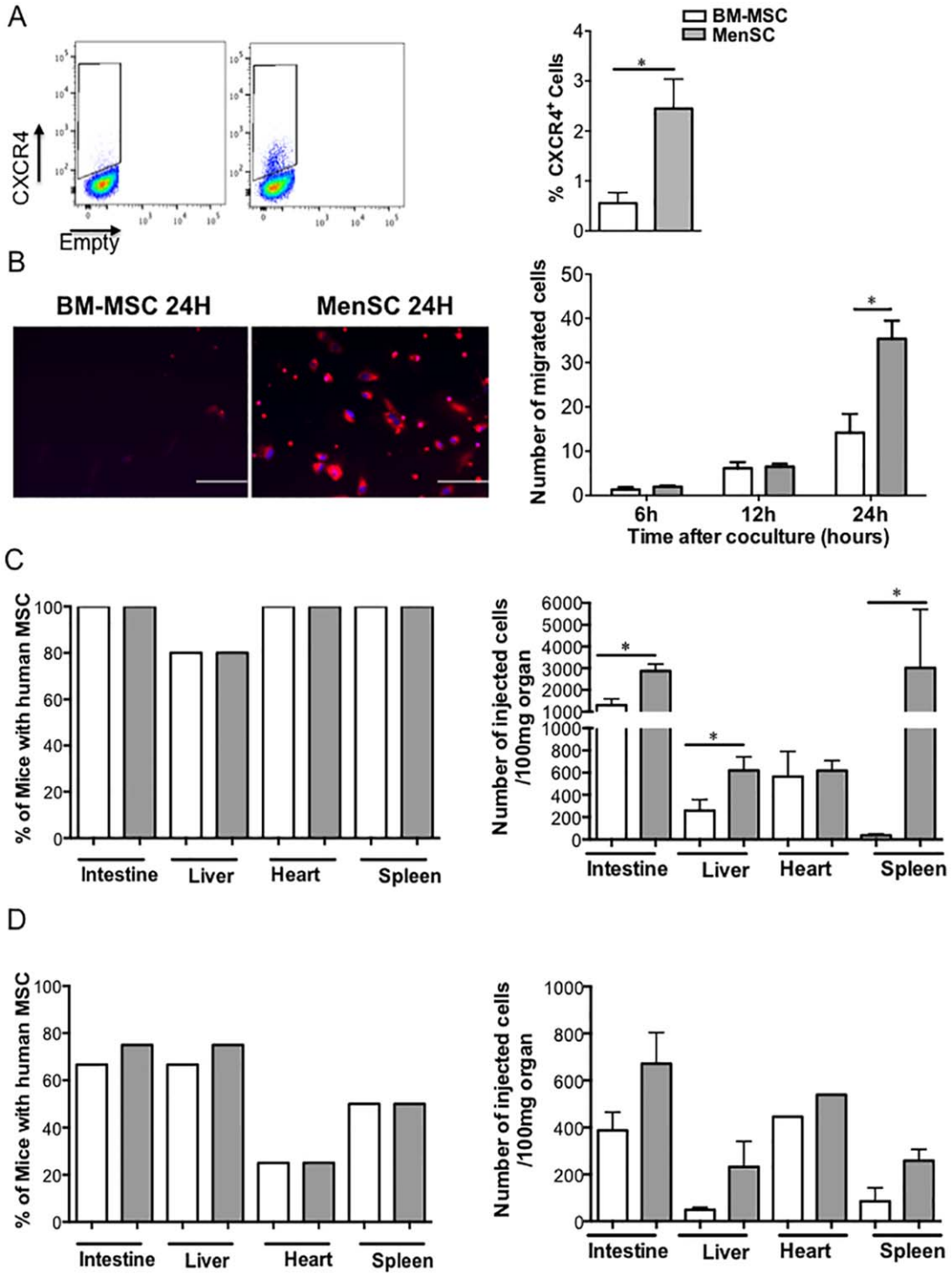

Figure 7. MenSCs exert a higher migratory potential than BM-MSCs. **(A)**: The expression level of CXCR4 was evaluated in BM-MSCs and MenSCs by fluorescence-activated cell sorting. **(B)**: The migratory capacities of both BM-MSCs and MenSCs were evaluated in vitro using a transwell system. The capacity of the cells to migrate in response to the serum used as a chemo attractant was evaluated after 6, 12, and 24 hours. The percentage and the number of MenSCs and BM-MSCs were quantified on NOD-scid IL2rγnull (NSG) mice after irradiation. NSG mice were injected via intraperitoneal and the migratory and homing capacities of both BM-MSCs and MenSCs were evaluated after **(C)** 1 day or **(D)** 8 days after the injection by quantitative polymerase chain reaction using human ALU sequences. Results are represented as mean $\pm$ SEM using four MenSCs and three BM-MSCs donors for the transwell system experiment, and images are representative of migration after 24 hours (scale bars = 50 μm). For the biodistribution assay, four to five different mice were used per experimental group. *p* values represent the statistical significance between MenSCs and BM-MSCs. Abbreviations: BM-MSCs, bone marrow-derived mesenchymal stem cells; MenSC, MSCs isolated from menstrual fluids. *$p < 0.055$

inflammatory and proinflammatory effect depending on the PBMC:MenSCs cell ratio. This dual effect was in concordance with other studies reporting that high concentrations of BM-MSCs suppress alloreactive T cells, whereas low MSC concentrations stimulate lymphocyte proliferation [37–39]. At low concentrations, MenSCs were also less efficient to inhibit the induction of CD8 + T and $CD4^+$ Th1 lymphocytes. This reduced immunosuppressive capacity was associated with a lower induction of anti-inflammatory $IL\text{-}4^+IL\text{-}10^+CD4^+$ lymphocyte subset. Our data strongly demonstrated that MenSCs are less suppressive than BM-MSCs at low concentrations both on the proliferation and the differentiation of T-cell subsets.

The low immunosuppressive capacity of MenSCs may be related to the reduced basal expression of both IFNγR1 and IFNγR2, which likely impaired their activation by IFN-γ [22]. Consequently, the expression levels of several immunomodulatory molecules, such as IL-6, Cox2, Activin A, IDO activity, and PDL-1 were lower in MenSCs than in BM-MSCs. PD-L1 is an important mediator involved in the suppressive effect of MSCs as demonstrated with placental-and BM-derived MSCs [40–42]. IDO, COX2, and Activin A are other major suppressive mediators of human MSCs, which are also downregulated in MenSCs [18, 43, 44]. Indeed, the moderate immunosuppressive function of MenSCs is likely due to a reduced capacity to be activated by IFN-γ to release important mediators.

We confirmed the results observed in vitro, in the autoimmune CIA model. The CIA model offers a good opportunity to study arthritis progression after MSC implantation [33, 45]. In contrast to BM-MSCs, MenSCs failed to exhibit any therapeutic benefit in CIA progression. Additionally, mice treated with MenSCs as opposed to BM-MSCs were unable to decrease inflammatory Th1 and Th17 lymphocytes suggesting that MenSCs fail to improve CIA course, probably due to a diminished capacity to regulate the switch from a proinflammatory to an anti-inflammatory profile. To further confirm the lower suppressive activity of MenSCs, we relied on the use of another immune mediated disease model, the acute xeno-GVHD, as it presents the advantage to allow the study of the interactions between T-cells and MSCs, both from human origin [46, 47]. While both BM-MSCs and MenSCs improved the survival rates of mice, an interesting result of this study is that MenSCs-treated mice displayed higher survival rates compared to both BM-MSC and control groups. This was associated to histological improvement of the intestine structure by both BM-MSCs and MenSCs. Nevertheless, the difference could not be attributed to a higher suppressive function since only BM-MSCs were able to lower the number of human $CD45^+$ cells even though MenSCs upregulated and downregulated the expression of IFN-γ and IL-10, respectively.

The opposite effect of MenSCs in the GVHD model on tissue protection on one side, and proinflammation on the other side results in better survival rate. In order to explain these results, it is important to mention that the humanized GVHD animal model is established following a combination of two different stress sources including the high irradiation doses and the injection of total human PBMCs. It is well-documented that MSCs possess a high potential to repair and protect different healthy tissues against radiation damages in many animal models [48, 49]. Herein, MenSCs seemed to foster an important protective and regenerative effect compensating their immunosuppressive shortfall, resulting in a noticeable therapeutic effect in GVHD. This could be attributed to a superior paracrine response of MenSCs to hypoxic conditions by the secretion of VEGF and basic fibroblast growth factor (bFGF), and a higher capacity to generate blood vessels both in vitro and in vivo as we previously reported [13]. Moreover, we observed that only mice treated with MenSCs significantly increased the expression of human HGF and VEGF in the liver compared to control group. A possible explanation for this increased therapeutic effect in the GVHD model is that MenSCs migrate at a higher rate and display a better homing potency than BM-MSCs in vivo. Our results, are in line with the study that has shown that mice treated with MSCs overexpressing the migration molecule CXCR4 significantly increased the survival of GVHD through an enhanced migration potential [35]. Indeed, we demonstrated that the expression of CXCR4 was significantly higher in MenSCs than BM-MSCs and this was correlated with a superior migration rate of MenSCs in vitro. Furthermore, in a biodistribution assay our data demonstrated that MenSCs were able to migrate rapidly to the target organs 24 hours postinjection compared to BM-MSC. At 8 days postinjection, MenSCs were able to efficiently home into the intestine, spleen, and liver and in a higher rate than BM-MSCs. Importance of MSC migration and homing has been detailed in some studies and shown to improve animal survival in GVHD where inefficient migration, survival, and homing limits the therapeutic effect of MSCs in GVHD [35, 50]. Moreover, all of these factors are important properties that can explain the outcome observed in the GVHD model.

The present results raise a warning concerning therapeutic application of MenSCs in autoimmune diseases as rheumatoid arthritis. While they do not imply MenSCs are the first-line cell source for treatment for GVHD, they do suggest MenSCs might have higher protective effect following irradiation damage. Also the therapeutic effect of autologous versus allogeneic use of MenSCs needs to be considerate. This still requires further investigation in a more related animal model.

Conclusions

As many autologous and allogeneic clinical trials using MenSCs are being planned, the information provided here raises the awareness for assessing carefully their potential side effects and presents decisive arguments for the disqualification of their use in immune-mediated diseases. This represents a key prerequisite for securing the development of safe and effective cell therapies devoid of setbacks.

Disclosure of Potential Conflicts of Interest

Maroun Khoury is the CSO of Cells for Cells and REGENERO, Francisca Alcayaga-Miranda received stipends from Cells for Cells. The other authors indicate no potential conflicts of interest.

Acknowledgments

We thank Samy Silva and CCHEN for the technical assistance in the irradiation of mice; Paula Valenzuela and Consuelo Valenzuela for excellent technical assistance; Dr. Jorge

Bartolucci and Dr. Hugo Azocar for providing the patients samples; Macarena Ocaña and Claudia Rubí for help in animal models experiments and Marisa Teigell for helping on histological analysis. This work was funded by Cells for Cells S.A, the Chilean National Commission for Scientific and Technological Investigation (CONICYT), FONDEF IDeA Program, grant number CA12i10349 and the postdoctoral fellowship "Becas Chile" number 74140021. M.J.T. is part of the Biomedicine PhD program in the Universidad de los Andes, Santiago, Chile. This work was supported by Inserm, the University of Montpellier I and grants from the French National Research Agency as part of the "Investments for the Future" program n° ANR-11-INBS-0005 and funding from the European Community's seventh framework program for the collaborative project: "REGENER-AR:Bringing Regenerative Medicine into the market: Allogeneic eASCs Phase IB/IIA clinical trial for treating Rheumatoid Arthritis" (contract no. 279174 EC). We thank the "Réseau des Animaleries de Montpellier" animal facility, the "Réseau d'Histologie Expérimentale de Montpellier" histology facility for processing our animal tissues and the "Montpellier RIO Imaging" platform.

Author Contributions

P.L.C., M.J.T., F.D., D.N., and M.K.: conception and design, acquisition of data, and analysis and interpretation of data; P.L.C., M.J.T., G.T., K.T., F.A.M., and A.F.: performing the experiments and data analysis; P.L.C. and M.K.: prepared the manuscript; F.F., D.N., F.D., S.I., C.J., and M.K.: revised critically the manuscript. The final manuscript was read and approved by all authors. P.L-C. and M.J.T. contributed equally to this work.

References

1 Friedenstein AJ, Chailakhyan RK, Latsinik NV et al. Stromal cells responsible for transferring the microenvironment of the hemopoietic tissues. Cloning in vitro and retransplantation in vivo. Transplantation 1974;17:331–340.

2 Owen M, Friedenstein AJ. Stromal stem cells: Marrow-derived osteogenic precursors. Ciba Found Symp 1988;136:42–60.

3 Krampera M, Glennie S, Dyson J et al. Bone marrow mesenchymal stem cells inhibit the response of naive and memory antigen-specific T cells to their cognate peptide. Blood 2003;101:3722–3729.

4 Le Blanc K, Pittenger M. Mesenchymal stem cells: Progress toward promise. Cytotherapy 2005;7:36–45.

5 Le Blanc K, Ringden O. Immunomodulation by mesenchymal stem cells and clinical experience. J Internal Med 2007;262:509–525.

6 Lee JM, Jung J, Lee HJ et al. Comparison of immunomodulatory effects of placenta mesenchymal stem cells with bone marrow and adipose mesenchymal stem cells. Int Immunopharmacol 2012;13:219–224.

7 Lupu M, Khalil M, Andrei E et al. Integration properties of Wharton's jelly-derived novel mesenchymal stem cells into ventricular slices of murine hearts. Cell Physiol Biochem 2011;28:63–76.

8 Mosna F, Sensebe L, Krampera M. Human bone marrow and adipose tissue mesenchymal stem cells: A user's guide. Stem Cells Dev 2010;19:1449–1470.

9 Mitrano TI, Grob MS, Carrion F et al. Culture and characterization of mesenchymal stem cells from human gingival tissue. J Periodontol 2010;81:917–925.

10 Ulrich D, Muralitharan R, Gargett CE. Toward the use of endometrial and menstrual blood mesenchymal stem cells for cell-based therapies. Expert Opin Biol Ther 2013;13:1387–1400.

11 Zhong Z, Patel AN, Ichim TE et al. Feasibility investigation of allogeneic endometrial regenerative cells. J Transl Med 2009;7:15.

12 Meng X, Ichim TE, Zhong J et al. Endometrial regenerative cells: A novel stem cell population. J Transl Med 2007;5:57.

13 Alcayaga-Miranda F, Cuenca J, Luz-Crawford P et al. Characterization of menstrual stem cells: Angiogenic effect, migration and hematopoietic stem cell support in comparison with bone marrow mesenchymal stem cells. Stem Cell Res Ther 2015;6:32.

14 Bozorgmehr M, Moazzeni SM, Salehnia M et al. Menstrual blood-derived stromal stem cells inhibit optimal generation and maturation of human monocyte-derived dendritic cells. Immunol Lett 2014;162:239–246.

15 Aggarwal S, Pittenger MF. Human mesenchymal stem cells modulate allogeneic immune cell responses. Blood 2005;105:1815–1822.

16 Djouad F, Charbonnier LM, Bouffi C et al. Mesenchymal stem cells inhibit the differentiation of dendritic cells through an interleukin-6-dependent mechanism. Stem Cells 2007;25:2025–2032.

17 Spaggiari GM, Capobianco A, Abdelrazik H et al. Mesenchymal stem cells inhibit natural killer-cell proliferation, cytotoxicity, and cytokine production: Role of indoleamine 2,3-dioxygenase and prostaglandin E2. Blood 2008;111:1327–1333.

18 English K, Ryan JM, Tobin L et al. Cell contact, prostaglandin E(2) and transforming growth factor beta 1 play non-redundant roles in human mesenchymal stem cell induction of CD4+CD25(High) forkhead box P3 + regulatory T cells. Clin Exp Immunol 2009;156:149–160.

19 Luan XY, Liu XB. [Comparison the inhibitory effects of human bone marrow mesenchymal stem cells and human placenta mesenchymal stem cells on T cell proliferation]. Xi bao yu fen zi mian yi xue za zhi = - Chin J Cell Mol Immunol 2010;26:849–851.

20 Djouad F, Jackson WM, Bobick BE et al. Activin A expression regulates multipotency of mesenchymal progenitor cells. Stem Cell Res Ther 2010;1:11.

21 Krampera M, Cosmi L, Angeli R et al. Role for interferon-gamma in the immunomodulatory activity of human bone marrow mesenchymal stem cells. Stem Cells 2006;24:386–398.

22 Schurgers E, Kelchtermans H, Mitera T et al. Discrepancy between the in vitro and in vivo effects of murine mesenchymal stem cells on T-cell proliferation and collagen-induced arthritis. Arthritis Res Ther 2010;12:R31.

23 Tobin LM, Healy ME, English K et al. Human mesenchymal stem cells suppress donor CD4(+) T cell proliferation and reduce pathology in a humanized mouse model of acute graft-versus-host disease. Clin Exp Immunol 2013;172:333–348.

24 Carrion F, Nova E, Ruiz C et al. Autologous mesenchymal stem cell treatment increased T regulatory cells with no effect on disease activity in two systemic lupus erythematosus patients. Lupus 2010;19:317–322.

25 Bouffi C, Bony C, Courties G et al. IL-6-dependent PGE2 secretion by mesenchymal stem cells inhibits local inflammation in experimental arthritis. PloS One 2010;5:e14247.

26 Wuchter P, Bieback K, Schrezenmeier H et al. Standardization of Good Manufacturing Practice-compliant production of bone marrow-derived human mesenchymal stromal cells for immunotherapeutic applications. Cytotherapy 2015;17:128–139.

27 Grayson WL, Bunnell BA, Martin E et al. Stromal cells and stem cells in clinical bone regeneration. Nat Rev Endocrinol 2015;11:140–150.

28 Dominici M, Le Blanc K, Mueller I et al. Minimal criteria for defining multipotent mesenchymal stromal cells. The International Society for Cellular Therapy position statement. Cytotherapy 2006;8:315–317.

29 Djouad F, Bony C, Haupl T et al. Transcriptional profiles discriminate bone marrow-derived and synovium-derived mesenchymal stem cells. Arthritis Res Ther 2005;7:R1304–1315.

30 Luz-Crawford P, Tejedor G, Mausset-Bonnefont AL et al. Glucocorticoid-induced leucine zipper governs the therapeutic potential of mesenchymal stem cells by inducing a switch from pathogenic to regulatory Th17 cells in a mouse model of collagen-induced arthritis. Arthritis Rheumatol 2015;67:1514–1524.

31 Alex P, Zachos NC, Nguyen T et al. Distinct cytokine patterns identified from multiplex profiles of murine DSS and TNBS-induced colitis. Inflam Bowel Dis 2009;15:341–352.

32 Toupet K, Maumus M, Peyrafitte JA et al. Long-term detection of human adipose-derived mesenchymal stem cells after intraarticular injection in SCID mice. Arthritis Rheum 2013;65:1786–1794.
33 Gonzalez MA, Gonzalez-Rey E, Rico L et al. Treatment of experimental arthritis by inducing immune tolerance with human adipose-derived mesenchymal stem cells. Arthritis Rheum 2009;60:1006–1019.
34 Kallmeyer K, Pepper MS. Homing properties of mesenchymal stromal cells. Exp Opin Biol Ther 2014:1–3.
35 Chen W, Li M, Li Z et al. CXCR4-transduced mesenchymal stem cells protect mice against graft-versus-host disease. Immunol Lett 2012;143:161–169.
36 Nikoo S, Ebtekar M, Jeddi-Tehrani M et al. Effect of menstrual blood-derived stromal stem cells on proliferative capacity of peripheral blood mononuclear cells in allogeneic mixed lymphocyte reaction. J Obstetrics Gynaecol Res 2012;38:804–809.
37 Le Blanc K, Tammik L, Sundberg B et al. Mesenchymal stem cells inhibit and stimulate mixed lymphocyte cultures and mitogenic responses independently of the major histocompatibility complex. Scand J Immunol 2003;57:11–20.
38 Fang L, Lange C, Engel M et al. Sensitive balance of suppressing and activating effects of mesenchymal stem cells on T-cell proliferation. Transplantation 2006;82:1370–1373.
39 Bocelli-Tyndall C, Bracci L, Schaeren S et al. Human bone marrow mesenchymal stem cells and chondrocytes promote and/or suppress the in vitro proliferation of lymphocytes stimulated by interleukins 2, 7 and 15. Ann Rheum Dis 2009;68:1352–1359.
40 Zhou Q, Munger ME, Veenstra RG et al. Coexpression of Tim-3 and PD-1 identifies a CD8 + T-cell exhaustion phenotype in mice with disseminated acute myelogenous leukemia. Blood 2011;117:4501–4510.
41 Wang G, Zhang S, Wang F et al. Expression and biological function of programmed death ligands in human placenta mesenchymal stem cells. Cell Biol Int 2013;37:137–148.
42 Luz-Crawford P, Kurte M, Bravo-Alegria J et al. Mesenchymal stem cells generate a CD4+CD25+Foxp3 + regulatory T cell population during the differentiation process of Th1 and Th17 cells. Stem Cell Res Ther 2013;4:65.
43 Chatterjee D, Marquardt N, Tufa DM et al. Human umbilical cord-derived mesenchymal stem cells utilize Activin-A to Suppress Interferon-gamma production by natural killer cells. Front Immunol 2014;5:662.
44 Jones BJ, Brooke G, Atkinson K et al. Immunosuppression by placental indoleamine 2,3-dioxygenase: A role for mesenchymal stem cells. Placenta 2007;28:1174–1181.
45 Chen M, Su W, Lin X et al. Adoptive transfer of human gingiva-derived mesenchymal stem cells ameliorates collagen-induced arthritis via suppression of Th1 and Th17 cells and enhancement of regulatory T cell differentiation. Arthritis Rheum 2013;65:1181–1193.
46 Ito R, Katano I, Kawai K et al. Highly sensitive model for xenogenic GVHD using severe immunodeficient NOG mice. Transplantation 2009;87:1654–1658.
47 Gregoire-Gauthier J, Selleri S, Fontaine F et al. Therapeutic efficacy of cord blood-derived mesenchymal stromal cells for the prevention of acute graft-versus-host disease in a xenogenic mouse model. Stem Cells Dev 2012;21:1616–1626.
48 Linard C, Busson E, Holler V et al. Repeated autologous bone marrow-derived mesenchymal stem cell injections improve radiation-induced proctitis in pigs. Stem Cells Transl Med 2013;2:916–927.
49 Hu KX, Sun QY, Guo M et al. The radiation protection and therapy effects of mesenchymal stem cells in mice with acute radiation injury. Br J Radiol 2010;83:52–58.
50 Li H, Jiang Y, Jiang X et al. CCR7 guides migration of mesenchymal stem cell to secondary lymphoid organs: A novel approach to separate GvHD from GvL effect. Stem Cells 2014;32:1890–1903.


See www.StemCells.com for supporting information available online.